Supplementary Information

Yesenia A García Jomaso,[1,1] Brenda Vargas,[1,1] David Ley Domínguez,[1,1] Román Armenta,[1,1] Huziel E. Sauceda,[1,1] César L Ordoñez-Romero,[1,1] Hugo A Lara-García,[1,1] Arturo Camacho-Guardian,[1,1] and Giuseppe Pirruccio[1,1]

[1] *Instituto de Física, Universidad Nacional Autónoma de México, Apartado Postal 20-364, Ciudad de México C.P. 01000, Mexico*

(Dated: August 25, 2023)

I. Λ-SCHEME: THEORETICAL DETAILS

We consider the imaginary-time Green's function defined as $\mathcal{G}_{\alpha,\beta}(\tau) = -\langle T_\tau[\hat{\psi}_\alpha(\tau)\hat{\psi}^\dagger_\beta(0)]\rangle$, here the subindices α, β correspond to the left/right cavity photon and exciton, respectively. The Dyson's equation $\mathcal{G}^{-1}(z) = [\mathcal{G}^{(0)}(z)]^{-1} - \Sigma(z)$, is given in terms of the ideal $\mathcal{G}^{(0)}(z)$ Green's function which define a diagonal matrix

$$\mathcal{G}^{(0)}_{11}(z) = \frac{1}{z - \omega^L_c(\theta)}, \qquad \mathcal{G}^{(0)}_{22}(z) = \frac{1}{z - \omega^R_c(\theta)} \qquad \mathcal{G}^{(0)}_{33}(z) = \frac{1}{z - \omega_X}. \tag{1}$$

The self-energy gives the coupling between the left and right cavity photons $\Sigma_{12}(z) = \Sigma_{12}(z) = -t$, with t the tunneling coefficient. The light-matter coupling between the excitons and right cavity photons is given by $\Sigma_{23}(z) = \Sigma_{32}(z) = \Omega$.

In this case, as mentioned in the main text, the Green's function acquires an analytical form, in particular, the Green's function of the left cavity photons is given by

$$\mathcal{G}_{11}(z) = \frac{1}{z - \omega^L_c(\theta) - \frac{t^2}{z - \omega^R_c(\theta) - \frac{\Omega^2}{z - \omega_X}}}. \tag{2}$$

If $\omega^R_c(\theta)$ is detuned from the exciton energy and following the branch of the middle polariton we obtain

$$\mathcal{G}_{11}(\omega_X + \omega) \approx \frac{1}{\omega_X + \omega - \omega^L_c(\theta) - \frac{t^2}{\Omega^2}(\omega)}. \tag{3}$$

The pole is found at

$$\omega(\theta) = \frac{[\omega^L_c(\theta) - \omega_X]}{1 + \left(\frac{t}{\Omega}\right)^2}, \tag{4}$$

that is, the energy of the middle polariton is given by $\omega_{\rm MP}(\theta) = \omega_X + \frac{[\omega^L_c(\theta) - \omega_X]}{1 + \left(\frac{t}{\Omega}\right)^2}$ as given in the main text. This holds as long as the energy shift remains within the energy window $|\omega(\theta)| \ll \frac{t^2}{|\omega_X - \omega^R_c|}$.

The broadening of the photon and exciton lines can be included via additional terms which account for the losses. Then, the experimental model departs from the idealized scenario discussed before. The broadening of the right cavity photons reduces the energy window $\frac{t^2}{\sqrt{(\gamma^R_c)^2 + |\omega_X - \omega^R_c|^2}}$, while the broadening of the exciton lines leads to imperfect slow-light where the right cavity photons remains coupled to the middle polariton even at resonance $\omega^R_c(\theta = 0) = \omega_X$. This coupling is small as long as $\sqrt{(\gamma^R_c)^2 + |\omega_X - \omega^R_c|^2} \ll t^2/\gamma_X$. We estimate the ratio

$$\frac{t^2}{(\gamma_X \sqrt{(\gamma^R_c)^2 + |\omega_X - \omega^R_c|^2})} \approx 10 - 50$$

that is, we expect to see clear signatures of slow-light with right cavity photons effectively decoupled from the middle polaritons under resonant conditions.

In Fig. 1 we show the spectral function at normal incidence of the left (a) and right (b) cavity photons as a function of the detuning $\delta = \delta_{LX}$. The vanishing value of the spectral function $A_{22}(\mathbf{0}, \omega)$ around zero detuning signals the full decoupling of the right cavity photon from the middle polariton.

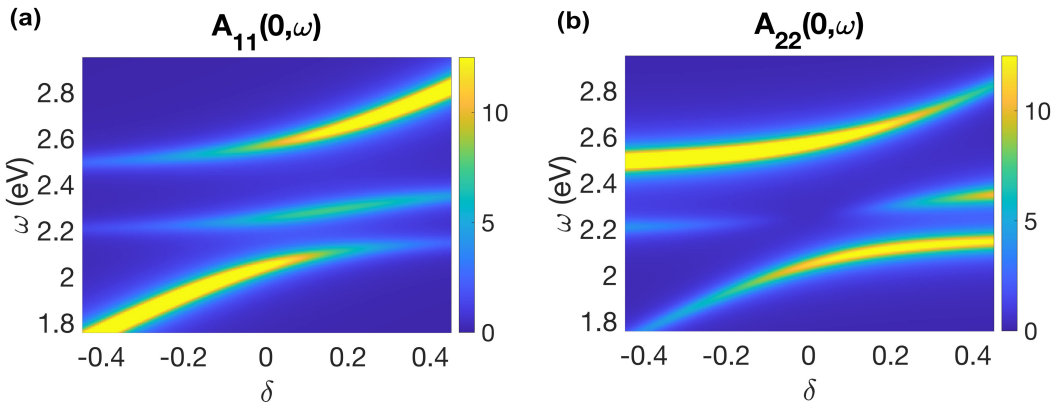

FIG. 1. Spectral function of the (a) Left and (b) Right cavity photons as a function of the left cavity detuning, $\delta = \delta_{LX}$. Around zero detuning we observe that the middle polariton decouples from the right cavity photon.

The vanishing of the right cavity photon component on the middle polariton is equivalent to the transparency window observed in electromagnetically induced transparency. This implies that the possibility to observe the middle polariton depends on the arrangement of the stacked cavities. In particular, we observe the middle polariton in reflectance as light is injected from the left cavity. If light were injected from the right cavity, then the reflectance spectrum would not signal the presence of this branch. For the same reason, transmittance would not reveal the MP branch. In this sense, the middle polariton is dark under certain circumstances.

II. EMERGENCE OF A FLATBAND

We now show additional experimental data that further illustrate the emergence of an intercavity polariton with a flatband dispersion. As explained in the main text, the polariton bands depend on the tunneling ratio, the Rabi splitting, and the different energy levels. We introduce the cavity detuning from the exciton energy at normal incidence $\delta_{LX} = \omega_c^{(L)}(\theta = 0) - \omega_X$ and $\delta_{RX} = \omega_c^{(R)}(\theta = 0) - \omega_X$.

Figures 2 (a)-(b) show the reflectance spectrum for varying detuning δ_{LX} with the remaining parameters as detailed in Table [1]. From left to right we observe the emergence of a purely middle intercavity polariton formed by a left cavity photon and an exciton localized in the right cavity. This is demonstrated by the quasiparticle residues shown in the bottom of Figs. 2 (a)-(b).

Fig. 4	δ_{LX}[eV]	δ_{RX}[eV]	t[eV]	2Ω[eV]	ω_X[eV]
a	-0.37	0.12	0.21	0.26	2.23
b	-0.18	0.09	0.21	0.26	2.23
c	-0.08	0.13	0.21	0.26	2.23
d	-0.03	0.13	0.21	0.26	2.23
e	0.00	0.17	0.23	0.245	2.25
f	0.07	0.15	0.21	0.26	2.23

Table 1. Theoretical parameters of the polariton branches in Fig. 2.

The evolution of the MP Hopfield coefficients illustrate that, as the left cavity detuning is driven to $\delta_{LX} = 0$, the right cavity photon decouples from the MP causing the suppression of its dispersion. For $\delta_{LX} = 0$, although the polariton energy matches the bare exciton, the MP does not loos its photonic character because it retains significant residue of the right cavity photon.

In Fig. 3 we show the evolution of the fluorescence as a function of the detuning. Pumping the system at $\omega_p = 2.62$eV ensures that for $\delta = \delta_{LX} = 0$ we drive coherently the UP which consists primarily of right cavity photons. The absence of the left photonic component in the driven UP strongly suppresses the emission of the MP for $\delta = \delta_{LX} = 0$

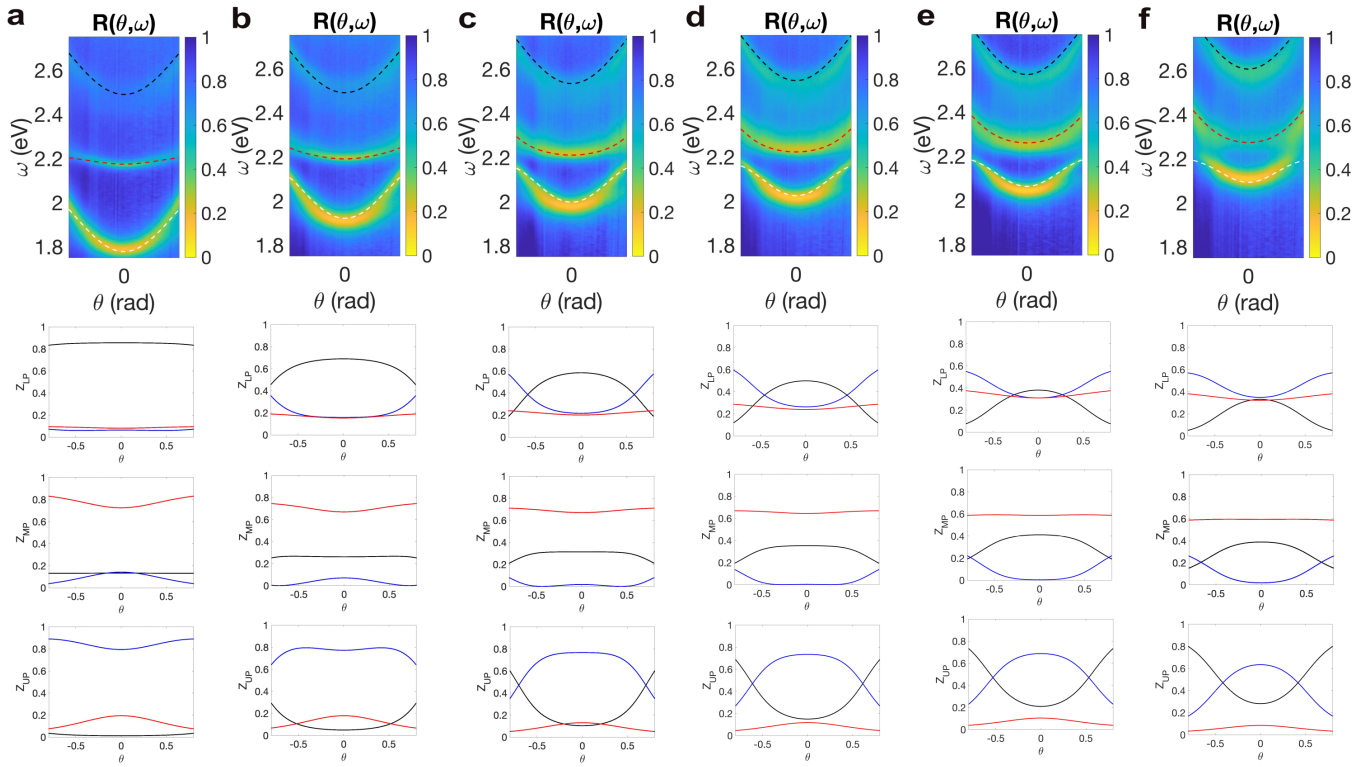

FIG. 2. s-polarized reflectance as a function of the incident angle and the energy for several cavity detunings. The dashed curves represent the energies of the three polariton branches, obtained with the parameters given in Table [1]. In the bootom row, we show the quasiparticle residues, i.e., the Hopfield coefficients, of the three quasiparticle branches following the color code of the main text.

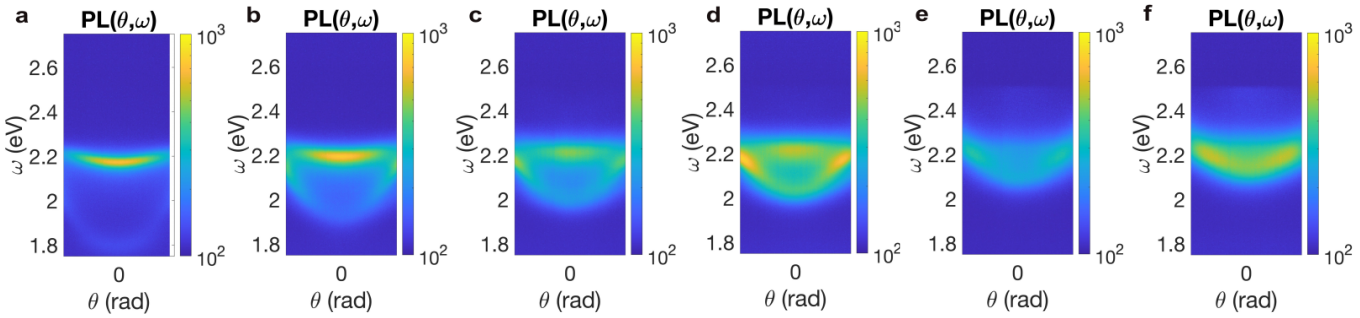

FIG. 3. s-polarized fluorescence for the same parameters as in Fig. 2 and Table 1. From left to right we observe a strong suppression of the MP fluorescence as the left cavity detuning approaches zero.

We should note that the right cavity photons are the dominant component of the UP in all of our cavity detunings. However, as we drive at $\omega_p = 2.62$eV, for large negative detuning, this driving is off-resonant, that is, it lies far above the energy of the upper polariton, and thus, photons are injected in left and right cavities. Therefore, for negative detunings, we observe emission from both the middle and lower polariton branches.

III. POLARITON DYNAMICS

In the main text we focus on the short-time dynamics of the polaritons. Here, we provide the experimental data in an extended time window. Figure 4 shows the LP (a) and MP (b) fluorescence decay for $\delta_{LX}/\text{eV} = -0.37$ (blue), on resonance $\delta_{LX}/\text{eV} = 0$ (purple) and $\delta_{LX}/\text{eV} = 0.20$ (green). The shaded pink area corresponds to the time window discussed in the main text where we focused on the initial decay. As a consequence of the coupling to the triplet state

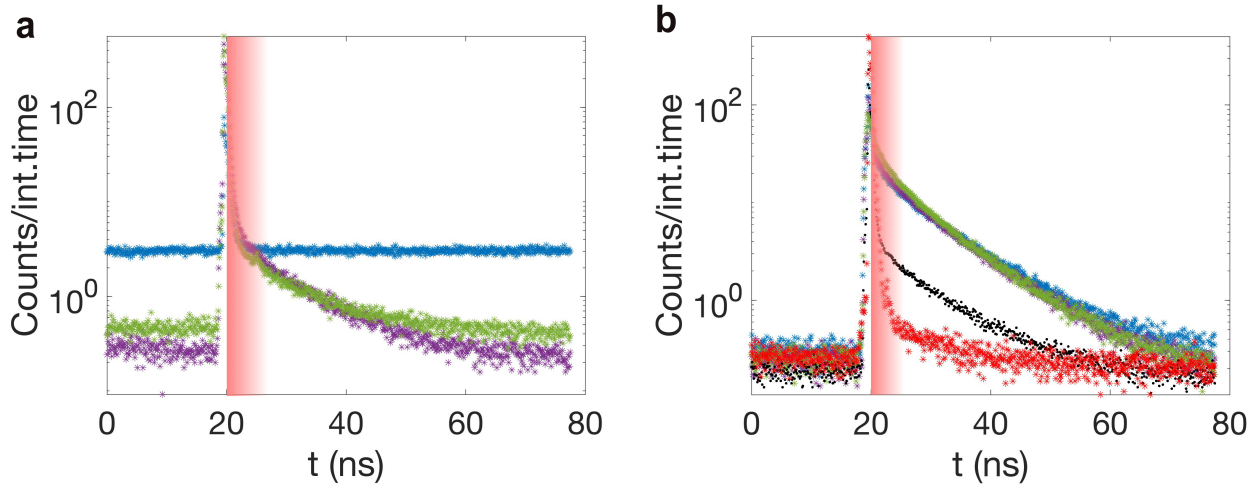

FIG. 4. Fluorescence decays of the LP (a) and MP (b) for different cavity detunings: $\delta_{LX}/\text{eV} = -0.37$ (blue), on resonance $\delta_{LX}/\text{eV} = 0.00$ (purple) and $\delta_{LX}/\text{eV} = 0.20$ (green). In (b), the black curve represents the decay of the ErB/PVA thin film in the absence of the cavity, while the red curve corresponds to the IRF. The shaded pink area corresponds to the time window discussed in the main text.

by intersystem crossing for large negative detunings, or to the bare exciton states for positive detunings, the decay of the LP for $t > 10$ns after the laser pulse arrival becomes more complex. In the former case, where the energy of the LP approaches the triplet state, we see the presence of a long-living state which does not decay entirely in the considered time window. A similar effect, although less pronounced, is seen as the LP shifts toward the bare exciton energy. An intermediate situation is observed for detunings around $\delta_{LX}/\text{eV} = -0.2$. The ability to control the dynamics of the LP was extensively discussed for a single cavity [1].

On the other hand, the MP energy lies very far away from the triplet state, thus the triplet state does not participate in the MP dynamics and its decay is given by the slow-light physics discussed in the main text. For $t > 10$ns after the laser pulse arrival, the MP time evolution resembles the dynamics of the ErB/PVA thin film in the absence of the cavity. This can be appreciated by comparing the black curve in Fig. 4(b) with the MP decays.

In Fig. 4(b) we show with red curve the IRF obtained by measuring a 0.5 M solution of ErB in water which is known to decay mono-exponentially with a lifetime well below the time resolution of our instrument. This choice ensures that the detector wavelength-dependent response does not play a role in our measurements. The same experimental conditions as for the cavity measurements are used. The full-width at half-maximum of this decay is approximately 350 ps. Having characterized the IRF curve, the short-time fit of the LP and MP decays can be safely conduct by excluding the first 600 ps after the intensity maximum. This time value is labelled as $t = 0$ ns in Fig.3(a) of our manuscript.

It is important to highlight that within the shaded pink area, i.e., within the first 10 ns from the arrival of the laser pulse, the dynamics of the ErB molecule in absence of the cavity can be excellently modeled by a single exponential. We find that $A = 0.9$, $\Gamma = 4.9$ ns^{-1} and $\eta = 0.24$ ns^{-1}. Thus the rich interplay observed for the MP and its overall slow dynamics cannot be account for with the ErB photophysics.

[1] Kati Stranius, Manuel Hertzog, and Karl Börjesson, "Selective manipulation of electronically excited states through strong light–matter interactions," Nature Communications **9**, 2273 (2018).